



1 Improving fire severity prediction in south-eastern Australia using 2 vegetation specific information

3 Kang He^{1,2}, Xinyi Shen³, Cory Merow^{2,4}, Efthymios Nikolopoulos⁵, Rachael V. Gallagher⁶, Feifei
4 Yang^{1,2}, Emmanouil N. Anagnostou^{1,2}

5 ¹Department of Civil and Environmental Engineering, University of Connecticut, Storrs, CT 06269, USA

6 ²Eversource Energy Center, University of Connecticut, Storrs, CT 06269, USA

7 ³School of Freshwater Sciences, University of Wisconsin, Milwaukee, Milwaukee, WI, 53204, USA

8 ⁴Department of Ecology and Evolutionary Biology, University of Connecticut, Storrs, CT 06269, USA

9 ⁵Department of Civil and Environmental Engineering, Rutgers University, Piscataway, NJ 08854, USA

10 ⁶Department of Biological Sciences, Macquarie University, North Ryde, NSW 2109, Australia

11 *Correspondence to:* Emmanouil N. Anagnostou (emmanouil.anagnostou@uconn.edu)

12 **Abstract.** Wildfire is a critical ecological disturbance in terrestrial ecosystems. Australia, in particular, has experienced
13 increasingly large and severe wildfires over the past two decades while globally fire risk is expected to increase significantly
14 due to the projected increase in fire weather severity and drought condition. Therefore, understanding and predicting fire
15 severity is critical for evaluating current and future impacts of wildfires on ecosystems. Here, we firstly introduce a vegetation-
16 type specific fire severity classification applied on satellite imagery, which is further used to predict fire severity using
17 antecedent drought conditions, fire weather, and topography of the fire season. Based on a ‘leave-one-out’ cross-validation
18 experiment, we demonstrate high accuracy for both the fire severity classification and the regression using a suite of
19 performance metrics: determination coefficient (R^2), mean absolute error (MPE) and root mean square error (RMSE), which
20 are 0.89, 0.05, and 0.07, respectively. Our results also show that the fire severity prediction results using the vegetation-type
21 specific thresholds could better capture the spatial patterns of fire severity, and has the potential to be applicable for seasonal
22 fire severity forecasting due to the availability of seasonal forecasts of the predictor variables.

23 **Keywords:** Fire severity; Normalized Burning Ratio; Random Forest; Vegetation type; Severity classification.

24 1 Introduction

25 Fire is recognized as a critical disturbance in ecosystems, which shapes vegetation across several continents (Archibald et al.,
26 2013; Gill, 1975; Giglio et al., 2010; Gomez et al., 2015). In recent decades, wildfires have affected extensive areas in forests
27 and woodlands across the globe, including those in Australia where over 10 million hectares were burned in the 2019-2020
28 fire season (Gallagher et al. 2021). These fires are considered unprecedented in contemporary Australian fire history (Nolan
29 et al., 2020; Shine, 2020), and more severe fires are expected in the future due to the impacts of climate change on fire-weather
30 and dynamics (Hennessy et al., 2005). Changes in fire conditions are also anticipated globally (Abatzoglou et al. 2019).
31 Therefore, predicting fire characteristics – such as severity – will be essential for evaluating current and future impact of
32 wildfires on ecosystems worldwide.



33 Fire severity, defined here as the magnitude of change in vegetation associated with fire, is routinely used to describe the
34 impact of wildfires on vegetation, soil and wildlife (Lentile et al. 2006; Keeley 2009). Field survey and remote sensing-based
35 evaluations of burn severity are commonly used by fire scientists and managers. Field survey-based evaluations involve
36 assessing the amount of biomass consumed (Keeley, 2009), measuring the changes in vegetation height (Wang and Glenn,
37 2009) or surface fuel consumption (Boby et al., 2010; Hudak et al., 2013). By contrast, remotely sensed evaluations of burn
38 severity use satellite imagery to quantify the magnitude of vegetation changes between pre-fire and post-fire conditions, in
39 terms of the changes in surface reflectance (Holden et al., 2009; Miller et al., 2009; Soverel et al., 2010) (e.g. the difference
40 between pre- and post-fire Normalized Burn Ratio (dNBR)).

41 Statistical approaches, which incorporate factors such as topography, weather and water availability provide insight into
42 possible drivers of fire severity (Morgan et al., 2014). For instance, Bradstock et al. (2010) investigated the effects of weather,
43 fuel and terrain on fire severity in south-eastern Australia. They found weather was the predominant influence on fire severity
44 while the influence of terrain was stronger under moderate conditions. Similarly, a study by Collins et al. (2013) examined the
45 relationships between environmental variables (i.e., fire weather, topography and fuel age) and fire severity in south-eastern
46 Australia and whether it can be modified by increasing mean annual precipitation. They concluded that the relationships
47 between crown fire and weather, topography and fuel age were largely unaltered across the precipitation gradient. Collins et
48 al. (2019) also examined the relative effect of fire weather, drought severity and landscape features (i.e., topography, fuel age,
49 vegetation type) on the occurrence of fire refugia in south-eastern Australia. They found that the fire weather and drought
50 severity were the primary drivers of the occurrence of fire refugia, moderating the effect of landscape attributes. Furthermore,
51 Clarke et al. (2014) investigated fire severity control factors, including landscape/vegetation or weather, providing evidence
52 that even though strong weather controls, fire history, terrain and vegetation shape the immediate effect. In addition, Bowman
53 et al. (2021) demonstrated that overwhelming dominance of fire weather in driving complete scorch or consumption of forest
54 canopies in natural and plantation forests in the 2019-20 megafires.

55 Despite the emerging evidence that statistical modelling with multiple biophysical and environmental predictor variables can
56 provide high accuracy estimates of fire severity, this technique is not widely adopted in major areas of known fire risk. One
57 such region is the southeast coast of Australia which is subject to annual fire seasons vary in extent and severity and has a high
58 richness of endemic plant species adapted to particular fire regimes (Gallagher et al., 2021). Besides, an accurate representation
59 of fire severity levels is important for managing and mitigating the effects of wildfires, both in terms of emergency response
60 and long-term ecological recovery. The most prevailing dNBR-based classification scheme, which rely on establishing the
61 relationship between in-situ measured Composite Burn Index (Key and Benson, 2006; Lutes et al., 2006) and satellite derived
62 dNBR, is designed only for certain regions and for limited vegetation types under certain climate (Eidenshink et al., 2007;
63 Keeley et al., 2009; Tran et al., 2018). While for the southeast coast of Australia, which is subject to annual wildfire seasons
64 and varies greatly in vegetation types with high richness of endemic plant species adapted to particular fire regimes (Gallagher
65 et al., 2021), no fire severity classification scheme exists.



66 Understanding current and predicting future fire severity in eastern Australia is critical for evaluating the potential for increased
67 extinction risk due to recurrent high severity fires (Enright et al. 2015) and is important for supporting ecologically informed
68 fire management (Clarke et al. 2019). Therefore, the predictor variables involved in the fire severity model should be accessible
69 for both historical events and projected future events (e.g. seasonal, climate).

70 In this study, we newly propose a vegetation specific fire severity classification scheme for predicting fire severity and
71 demonstrate its performance across the Australian state of New South Wales (NSW). Using drought conditions, vegetation
72 type, and fire weather conditions during the fire season as input, our modelling approach applies the Random Forest (RF)
73 classification method to predict the dNBR – an indicator of burn severity derived from Landsat imagery. We demonstrate
74 model performance based on 20 years of wildfire data from NSW through a leave-one-year-out cross-validation experiment.

75 2 Study area

76 New South Wales (NSW) in south-eastern Australia (Figure 1) occupies a subtropical-temperate climate region with relatively
77 mild weather and distinctive seasons (e.g., hot summers and cold winters) (Speer et al., 2009). Mean annual and extreme
78 temperatures are highest in the northwest of the state whereas average maximum temperatures in coastal areas range from
79 26 °C to 16 °C, while the average minimum temperature falls between 19 ° and 7 °C. There is a strong precipitation gradient
80 from east to west across the state, with annual precipitation on the eastern coast ranging between 600 mm/year and 1200
81 mm/year decreasing to generally less than 180 mm/year in the north west of the state
82 Vegetation across the study region is predominantly wet and dry sclerophyll forests, although is interspersed with areas of
83 rainforest, woodlands and coastal heath (Keith 2004).

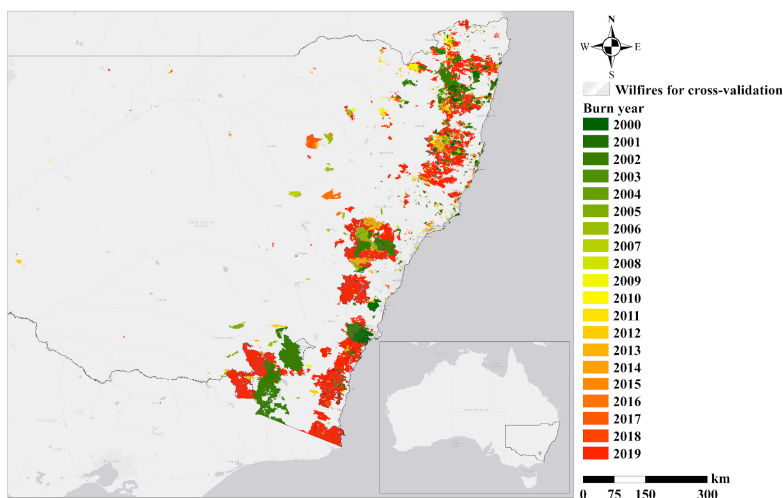


Figure 1. Locations of study wildfires over New South Wales, Australia



84 **3 Data and method**

85 **3.1 Model Input and output**

86 **3.1.1 Fire extent**

87 The spatial extent of annual fires between 2000 to 2019 is accessed from the NSW National Parks and Wildlife Service
88 (NPWS) Fire History – Wildfire and Prescribed Burns dataset ([https://data.nsw.gov.au/data/dataset/1f694774-49d5-47b8-
89 8dd0-77ca8376eb04](https://data.nsw.gov.au/data/dataset/1f694774-49d5-47b8-8dd0-77ca8376eb04)), produced by the Department of Planning, Industry and Environment. The NPWS Fire History is a
90 spatial polygon layer, with each polygon recording the boundary, start date, end date, and burn area. We use the NPWS
91 polygons whose burn areas are greater than 1 km² as the mask to include only the fire impacted areas. While this dataset is
92 unlikely to be a complete record of all fire events, it represents the largest single repository of fire extent data in NSW.

93 **3.1.2 Fire severity**

94 As a widely used fire severity index, the dNBR is calculated by subtracting the post-fire NBR raster from the pre-fire NBR
95 raster as in Eq (1):

$$96 \quad dNBR = PrefireNBR - PostfireNBR \quad (1)$$

97 The formula of NBR is similar to the normalized difference vegetation index (NDVI), except that it uses near-infrared (NIR)
98 and shortwave-infrared (SWIR) bands, as written in Eq (2) (García and Caselles, 1991; Key and Benson, 2006). NBR can be
99 computed by the Thematic Mapper (TM) and Enhanced Thematic Mapper Plus (ETM+) sensors on using Band 7 as the short-
100 wave infrared (SWIR) and Band 4 for Landsat 4-7 and Band 5 for Landsat 8 as the near infrared (NIR) reflectance, respectively.

$$101 \quad NBR = \frac{NIR - SWIR}{NIR + SWIR} \quad (2)$$

102 We calculate the dNBR within the fire boundaries from Landsat archive imagery, using the start date and end date to determine
103 the pre-fire and post-fire dates. In this study, the pre-fire NBR (preNBR), is used as a proxy of the initial condition of
104 vegetation.

105

106 **3.1.3 Vegetation**

107 Vegetation composition and structure are expected to influence fire propagation and severity (Collins et al., 2007) and the
108 vegetation type is also used as a proxy for vegetation structure (Hammill et al., 2006). The dominant vegetation over NSW is
109 wet and dry sclerophyll forests (Keith 2004). Wet sclerophyll forests can be divided into two subgroups (the shrubby sub-
110 formation and the grassy sub-formation), which have a tall canopies dominated by Eucalyptus and a monophyllous understory
111 ([https://www.environment.nsw.gov.au/threatenedSpeciesApp/VegFormation.aspx?formationName=Wet+sclerophyll+forests
112 +\(grassy+sub-formation\)](https://www.environment.nsw.gov.au/threatenedSpeciesApp/VegFormation.aspx?formationName=Wet+sclerophyll+forests+(grassy+sub-formation))). Two sub-formations of dry sclerophyll forests also occur: shrub/grass and shrubby. This study
113 focuses on burn severity for the dominant sclerophyll forests (Figure 1). The vegetation map is intersected with NPWS



114 polygons to identify the areas where sclerophyll forests have previously burned. The preNBR is derived from Landsat and
115 Sentinel-2 imageries.

116 3.1.3 Topography

117 Prior studies report strong control of topography on burn severity, by influencing fire behavior, fuel moisture, and water
118 balances (Fang et al., 2018, Harris and Taylor, 2015, Holden et al., 2009). Therefore, , we include three topographic measures
119 from Shuttle Radar Topography (SRTM, <https://www2.jpl.nasa.gov/srtm/world.htm>) DEM, elevation (DEM), slope (Slope),
120 and exposure (Exposure). Exposure represents the maximum amount of sunlight received at a grid based on topography, which
121 influences the moisture content of fuels and may influence the growth of vegetation. Exposure is calculated using the solar
122 radiation function in ArcMap 10.8.

123 3.1.3 Weather

124 Besides fuel and topography, weather is another important component of a wildfire environment. The McArthur Forest Fire
125 Danger Index (FFDI, McArthur 1967) is an empirical relationship comprising the short-term meteorological conditions and
126 the long-term drought factor (Dowdy et al. 2009). The FFDI is currently used operationally by the Australian Bureau of
127 Meteorology (BoM) to produce fire weather warnings to authorities, which is defined as:

$$128 \quad FFDI = 2 \times e^{(-0.45+0.897 \ln DF - 0.0345 RH + 0.038 T + 0.0234 V)} \quad (3)$$

129 where DF is the drought factor; and RH, T and V represent the relative humidity, surface air temperature and wind velocity,
130 respectively. In this study, we extract daily temperature, relative humidity and wind speed data from the ERA5-Land global
131 dataset over the burn areas (<https://cds.climate.copernicus.eu/cdsapp#!/dataset/reanalysis-era5-land?tab=form>).

132 The DF is estimated using the Keetch–Byram Drought Index (KBDI, Keetch and Byram 1968). KBDI is a continuous reference
133 scale describing the dryness of the soil and duff layers. The index increases for each day without rain and decreases when it
134 rains. KBDI is world widely used for drought monitoring for national weather forecast, wildfire prevention. KBDI over burnt
135 areas can be accessed in Takeuchi et al. (2015). The daily FFDI and KBDI values one day before the wildfires start are used
136 as the predictors in predicting burn severity.

137 3.2 Method

138 We newly propose an alternative way to determine the optimal thresholds in fire severity classification for different vegetation
139 types. The dNBR of all burnt pixels for each vegetation type are collected and a set of dNBR values at the quantiles from 0.05
140 to 0.95 are used as candidates of thresholds for fire severity classification. Secondly, a fire severity prediction model is
141 developed for each severity category based on the fire severity classification results, to provide the numeric prediction of
142 dNBR.



143 3.2.1 Fire severity classification by RF

144 Random Forest is developed as an extension of the classification and regression tree (CART) to improve the accuracy and
145 stability of the CART model (Breiman 2001). The steps of the RF algorithm are briefly summarized as: (i) randomly generate
146 *n*tree bootstrap samples of the original data. The elements not selected are referred to as ‘out of bag’ (OOB) samples. (ii) for
147 each split, randomly select *m*_try predictors of the original predictors and choose the best predictor among the *m*_try predictors
148 to partition the data. (iii) predict new data (OOB elements) by averaging predictions of the *n*tree trees; and (iv) the OOB
149 samples are used to estimate the prediction error. The RF can also provide a measurement of variable importance. One of the
150 approaches is to look at the increase in the OOB estimate error when the specific predictor variable is randomly permuted and
151 other predictors are constant. The more the error increases, the more important the variable is. These variable importance
152 values are used to rank the predictors in terms of their relative contribution to the model. The RF model was generated using
153 the package randomforest in R (<https://cran.r-project.org/web/packages/randomForest/>).

154

155 3.2.2 Fire severity prediction by XGboost

156 For the regression model, we implement the Extreme Gradient Boosting (XGBoost) algorithm, one of the most popular
157 supervised machine learning algorithms proposed by Chen et al. (2015). XGBoost employs a gradient boosting framework
158 that iteratively trains a sequence of weak prediction models and combines them into a strong model. In addition to gradient
159 boosting, XGBoost implements several advanced features, including regularization techniques to prevent overfitting, parallel
160 processing to speed up training, and built-in support for missing data (Chen and Guestrin, 2016). In the XGBoost algorithm,
161 complex interactions are modeled, and other complexities such as missing values in the predictors are managed without almost
162 any loss of information. Selection of features is performed by a combination of parameters (e.g., number of iterations, learning
163 rate) and the unique combinations of each attribute in the training data set. The XGBoost model is generated using the package
164 xgboost in R (<https://cran.r-project.org/web/packages/xgboost/>).

165

166 3.2.3 Calibration and validation

167 To evaluate the model’s performance, we use “leave -one group-out” for training and validation. The fire samples from 2000
168 to 2019 are firstly divided into 20 subsets depending on the year the fire occurred, and this holdout method is repeated 20
169 times. Secondly, at each time, one of the 20 subsets is used as the testing set, and the remaining 19 subsets are put together to
170 form the training set. Thirdly, the average error across all 20 trials is computed. The advantage of this cross-validation method
171 is that it gives us an indication of how well the model would do when making new predictions for data it has not already seen.
172 For performance evaluation of multiclass event classification based on QWD, accuracy is expressed as the proportion of
173 correctly predicted events over all predicted events, which is calculated as Eq (4):

$$174 \text{ Accuracy} = \frac{\text{Number of correct predictions}}{\text{Number of all predictions}} \quad (4)$$



175 While precision is expressed as the proportion of events correctly predicted as label X (low, moderate, or high) over all events
176 predicted as label X (Eq (5)).

$$177 \quad \textit{Precision} = \frac{\textit{True Positive}}{\textit{True Positive} + \textit{False Positive}} \quad (5)$$

178 in which True Positive represents the situation both observation and prediction are labelled as X, False Positive represents
179 observation is not labelled as X but prediction as label X.

180 Recall is calculated as:

$$181 \quad \textit{Recall} = \frac{\textit{True Positive}}{\textit{True Positive} + \textit{False Negative}} \quad (6)$$

182 in which False Negative represents the situation observation is label X but prediction is not label X.

183 Combining metrics of Precision and Recall, the F1 Score is the harmonic mean of Precision and Recall. The F1 Score gives
184 equal weight to Precision and Recall. A maximized F1 Score could create a balanced classification model, and is calculated as
185 follows:

$$186 \quad \textit{F1 score} = 2 * \frac{\textit{Precision} * \textit{Recall}}{\textit{Precision} + \textit{Recall}} \quad (7)$$

187

188 The coefficient of determination (R^2) is used to measure how well the prediction agreed with the actual values. The formula
189 of R^2 is described as:

$$190 \quad R^2 = \frac{1}{n} \sum_{i=1}^n \frac{(o_i - \frac{\sum_{i=1}^n o_i}{n})(p_i - \frac{\sum_{i=1}^n p_i}{n})^2}{o_i p_i} \quad (8)$$

191 Where o_i and p_i represent the actual and predicted values for sample i ; n is the total number of samples. The higher R^2 indicates
192 better fit of the model predictions to the actual values with best value of 1.

193 The mean absolute error (MAE) the mean relative error, the lower MAE is, the better the model performed.

$$194 \quad \textit{MAE} = \frac{\sum_{i=1}^n |p_i - o_i|}{n} \quad (9)$$

195 The root mean square error (RMSE) is used to quantify the random component of the error. The lower RMSE indicates better
196 model performance.

$$197 \quad \textit{RMSE} = \sqrt{\frac{\sum_{i=1}^n (p_i - o_i)^2}{n}} \quad (10)$$

198

199 4 Results

200 4.1 Fire severity of burnt vegetation

201 Over the past 20 years, wildfire history databases managed by government agencies indicate that approximately 112,590 km²
202 have been recorded as affected by fires in NSW, of which, almost 53,830 km² burned during the 2019-20 megafires (Figure



203 2). This dataset indicates that the annual burn area is typically below 5,000 km², but in exceptional years such as 2002 and
204 2003, the affected area can reach more than 10,000 km². The affected area from the 2019-20 fires is approximately 10 times
205 larger than those in other years from 2004 to 2018.

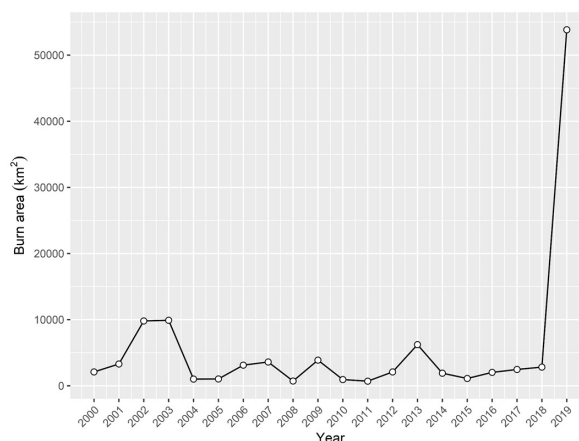


Figure 2. Annual burnt area (km²) across New South Wales, in south-eastern Australia.

206 Among the burnt area, the fractions of vegetation types are shown in Figure 2 (a). The dry sclerophyll forests (shrubby
207 subformation) accounted for the largest proportion of the burnt area (32.1%), followed by the dry sclerophyll forests
208 (shrub/grass subformation) which account for 16%. The wet sclerophyll forests (grassy subformation) occupy 14.2% of the
209 burnt area, while for the wet sclerophyll forests (shrubby subformation) the proportion is 11%. Specifically, the cleared area
210 accounted for 11.3% of the burnt area, approximately equal to those of the wet sclerophyll forests (shrubby subformation).
211 Other vegetation types largely affected by the wildfires are grassy woodlands, rainforest and heathlands, the proportion of
212 which are 6.7%, 2.5% and 2%, respectively. The distribution of fire severity indicated by dNBR for each vegetation type is
213 displayed as Figure 2 (b). These boxplots in Figure 2 (b) show that the fire severity varies significantly with vegetation type,
214 demonstrating that the vegetation specific thresholds should be applied in fire severity classification. For example, the fire
215 severity of cleared areas is overall the smallest while the fire severity of heathland shows the overall largest. The fire severity
216 varies even for the major vegetation type with different subgroups, for instance, the fire severity of dry sclerophyll forests with
217 shrubby subformation is larger than the fire severity of dry sclerophyll forests with shrub/grass subformation.
218

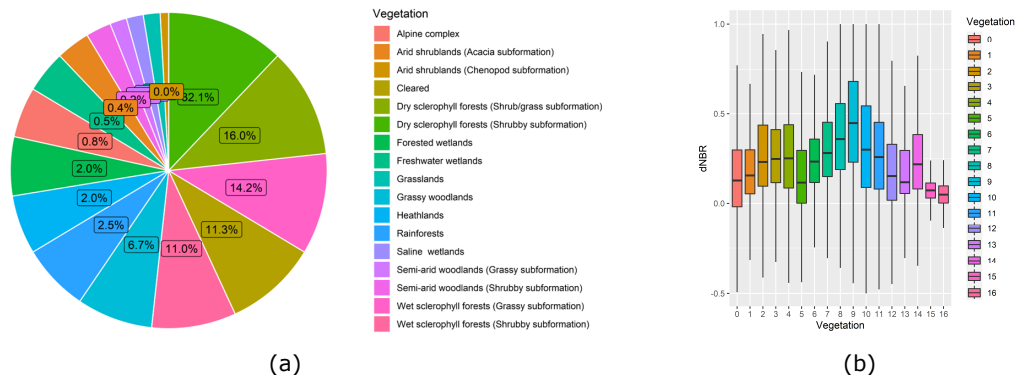


Figure 3. (a) The proportion of burnt area and (b) the distribution of fire severity grouped by vegetation type, over NSW from 2000 to 2019

219

220 4.2 Threshold determination for fire severity classification

221 Given the variability shown in Figure 2, we proposed an alternative way to determine the optimal thresholds in fire severity
 222 classification for different vegetation types. To determine these thresholds the dNBR of all burnt pixels for the vegetation type
 223 were collected and a set of dNBR values at the quantiles from 0.05 to 0.95 are used as the candidates of thresholds for the fire
 224 severity classification.

225 The classified samples using the threshold of dNBR at the quantiles are imported as the training set in RF models and the OOB
 226 estimate of error rate is recorded for the training samples. Figure 4 (a), (b), (c) and (d) show the variations of OOB estimate of
 227 error rate changes with thresholds of dNBR at the quantiles varying from 5% to 35% (low severity threshold)/35% to 65%
 228 (moderate severity threshold), when the high severity threshold are set as the dNBR values at the 65%, 75%, 85% and 95%
 229 quantiles, respectively. The optimal thresholds are determined when the lowest OOB estimate of error rate is found. For
 230 example, for dry sclerophyll forests (shrubby subformation), the thresholds for high, moderate and low severity classification
 231 are 0.55 (85% quantile), 0.38 (55%) and 0.20 (25%), respectively. Note that the classification step is merely used to improve
 232 the consecutive regression accuracy, rather than the final severity categorization result. The choice of threshold in this step
 233 therefore will not affect severity categorization. The categorization will be solely based on predicted severity value, using user
 234 defined thresholds.

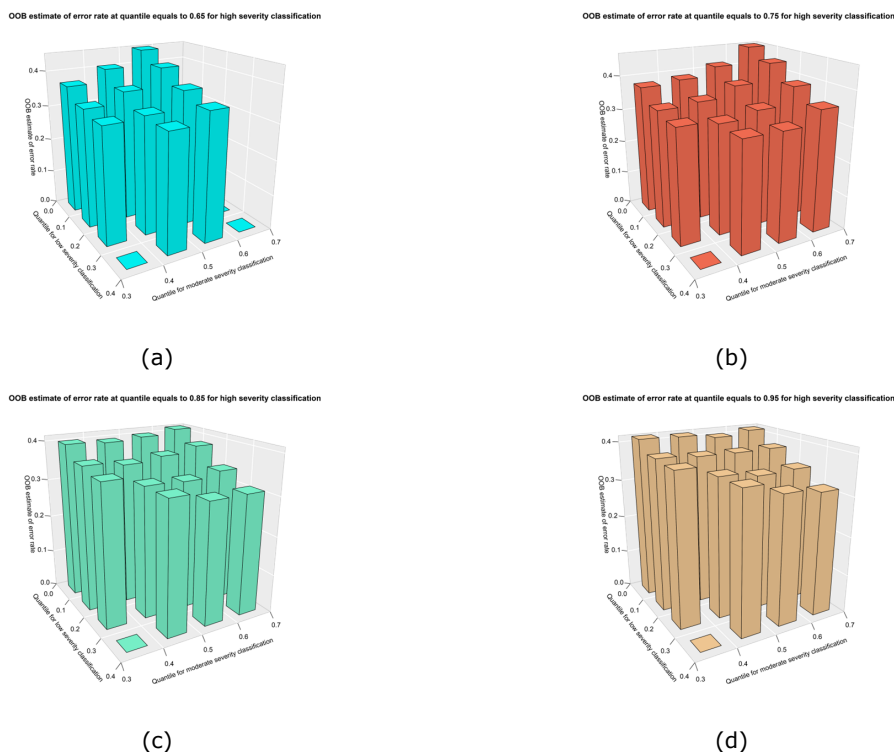


Figure 4. Variations of OOB estimate of error rate changes with thresholds of dNBR at the quantiles varying from 5% to 35% (low severity threshold)/35% to 65% (moderate severity threshold), when the high severity threshold are set as the dNBR values at the (a) 65%, (b) 75%, (c) 85% and (d) 95% quantiles.

235

236 The thresholds of dNBR for fire severity classification for different vegetation types are determined by the proposed method
237 and the results are presented in Table 1. It is shown that the thresholds vary significantly with vegetation type. For example,
238 for rainforests when dNBR of burnt area is around 0.20, this area should be classified as high severity. However, the burnt
239 area with the same dNBR (0.20) would be classified as moderate severity when wildfire burns over other vegetation types.
240 This difference is also found in the major vegetation type within different subgroups. A burn area with dNBR around 0.53
241 is classified as extreme high severity when fire burns over wet sclerophyll forests (grassy subformation), while this burn area is
242 classified as high severity when fire burns over wet sclerophyll forests (shrubby subformation). The differences in
243 classification thresholds are more significant between dry sclerophyll forests with shrub/grass subformation and shrubby
244 subformation. The thresholds for high severity classification are 0.44 and 0.55 for burnt area over dry sclerophyll forests
245 (shrub/grass subformation) and dry sclerophyll forests (shrubby subformation), respectively. These results indicate that using
246 the vegetation specific thresholds would obtain more reasonable fire severity classification results, while a lot of mis-



247 classifications are found when applying fixed thresholds in fire severity classification without considering the variations in
 248 vegetation cover.

249

250 Table 1. Thresholds of dNBR for fire severity classification by vegetation type.

Vegetation	Low	Moderate	High	Extreme
Rainforests	< 0.05 (25%)	0.05 - 0.18 (25%-45%)	0.18 - 0.41 (45%-75%)	> 0.41 (75%)
Wet sclerophyll forests (Shrubby subformation)	< 0.15 (35%)	0.15 - 0.34 (35%-55%)	0.34 - 0.56 (55%-85%)	> 0.56 (85%)
Wet sclerophyll forests (Grassy subformation)	< 0.17 (35%)	0.17 - 0.34 (35%-55%)	0.34 - 0.52 (55%-85%)	> 0.52 (85%)
Grassy woodlands	< 0.15 (35%)	0.15 - 0.36 (35%-55%)	0.36 - 0.55 (55%-85%)	> 0.55 (85%)
Dry sclerophyll forests (Shrub/grass subformation)	< 0.12 (15%)	0.12 - 0.26 (15%-45%)	0.26 - 0.44 (45%-75%)	> 0.44 (75%)
Dry sclerophyll forests (Shrubby subformation)	< 0.20 (25%)	0.20 - 0.38 (25%-55%)	0.38 - 0.55 (55%-85%)	> 0.55 (85%)
Heathlands	< 0.26 (35%)	0.26 - 0.40 (35%-55%)	0.40 - 0.57 (55%-75%)	> 0.57 (75%)

251

252 4.3 Fire severity prediction results

253 The performance of vegetation specific thresholds and the importance of vegetation type are validated by the cross-validation
 254 in the RF model. Figure 5 (a) and (b) show the relative importance of variables in the MF based on samples classified by
 255 vegetation specific thresholds and fixed thresholds, respectively. The error bar represents the standard deviation (sd) of relative
 256 importance in RF models in the cross-validation experiments. The preNBR is the most influential variable with relative
 257 importance around 28% and sd around 7%. The FFDI also plays an important role in the model with relative importance and
 258 sd of 21% and 6%, respectively. The KBDI shows close relative importance to those of FFDI, the values of mean relative
 259 importance and sd are 19% and 5% respectively. While for vegetation type, the relative importance (13%) is higher than those
 260 of topographic variables when the vegetation specific thresholds are applied. The sd of vegetation type is the largest (9%),
 261 owing to the differences in vegetation diversity in the training samples.

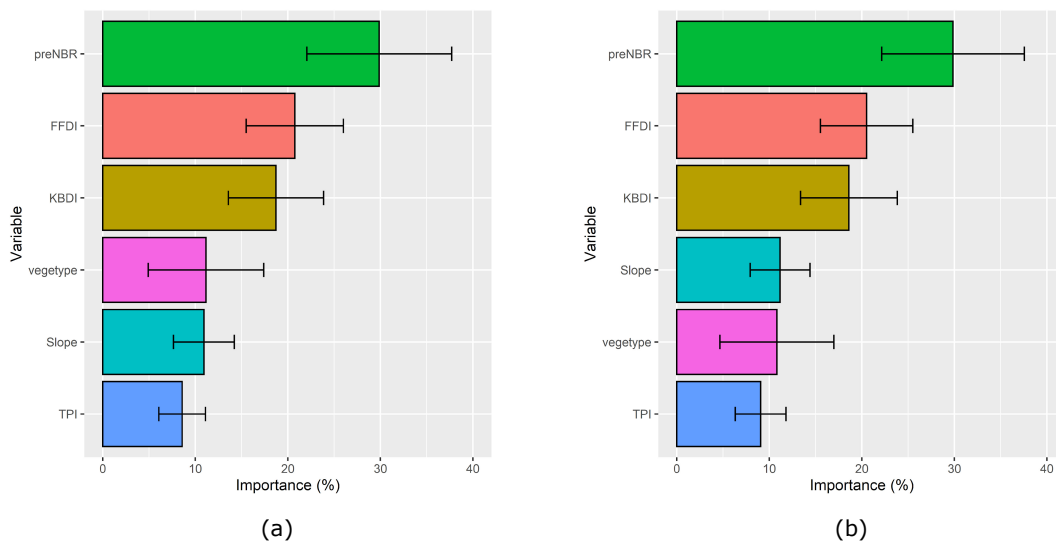


Figure 5. Relative importance of variables in RF models based on samples classified by (a) vegetation specific thresholds and (b) fixed thresholds.

262

263 The confusion matrix of the fire severity classification results is shown in Table 2. More samples are classified into extreme
 264 high severity classification when applying vegetation specific thresholds than those using fixed thresholds. Similarly, more
 265 samples are classified into low severity while implementing fixed thresholds than vegetation specific thresholds. This indicates
 266 that using fixed thresholds without considering the vegetation type tends to underestimate the fire severity levels. While for
 267 the performance of fire severity prediction, most events of extreme high severity are correctly identified by the RF model
 268 trained by samples classified by vegetation specific thresholds while more misclassified extreme high severity and high
 269 severity events are predicted by the RF model trained by samples classified by fixed thresholds.

270

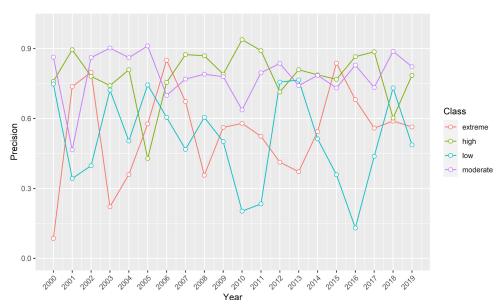
271 Table 2. Confusion matrix of prediction results based on RF model trained by samples classified by vegetation specific and
 272 fixed thresholds.

	Vegetation specific				Fixed				
	Extreme	High	Moderate	Low	Extreme	High	Moderate	Low	
Extreme	52680	22782	813	9	Extreme	36573	24573	1755	30
High	4749	94899	17265	171	High	3930	64740	21498	471
Moderate	501	20487	103536	3948	Moderate	852	19794	94857	8739
Low	147	1422	22239	36897	Low	357	2754	31299	70347

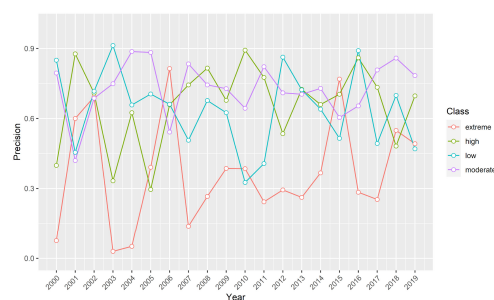
273



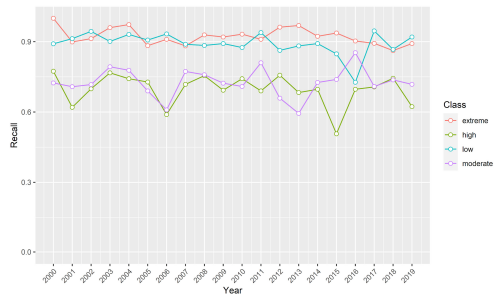
274 The overall classification accuracy calculated by equation (4) is 0.75 and 0.69, for RF models trained by samples classified by
275 vegetation specific and fixed thresholds, respectively. Figure 6 (a), (b) and (c) show the Precision, Recall and F1 score of event
276 severity classification results for each class label calculated by equations (5) – (7). The Accuracy, Precision, Recall results and
277 F1 Score close to 1 indicate accurate classification results. For the classification metrics of each class label, the high severity
278 events class exhibit the best Precision (0.85) relative to the moderate (0.76) and extreme high severity event classes (0.68),
279 while the Recall and F1 score for high severity events class are 0.64 and 0.73, respectively. The extreme high severity events
280 class exhibit the best Recall (0.89) relative to the other two classes, and the Precision and F1 score are 0.68 and 0.77,
281 respectively. The performances of fire severity classification are worse for the RF model trained by samples classified by the
282 fixed thresholds, with lower precision, recall and F1 score.



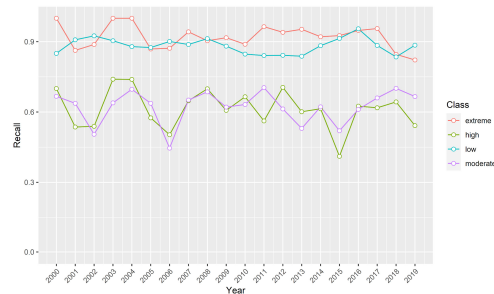
(a)



(b)



(c)



(d)

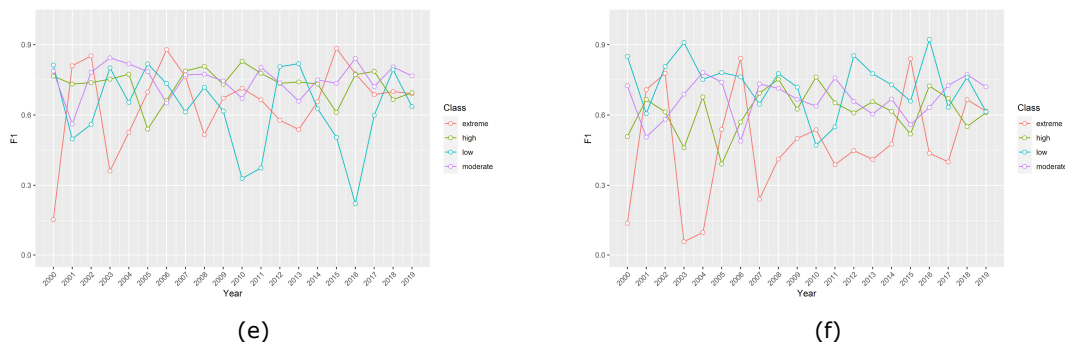


Figure 6. The results of Precision for predictions based on (a) vegetation specific thresholds and (b) fixed thresholds; The results of Recall for predictions based on (c) vegetation specific thresholds and (d) fixed thresholds; The results of F1 score for predictions based on (e) vegetation specific thresholds and (f) fixed thresholds;

283

284 Figure 7 displays the fire severity map for the 2002, 2008, 2011 and 2019 wildfires in NSW based on the vegetation specific
285 thresholds and fixed thresholds. It is obvious that the results using the fixed thresholds tend to underestimate the severity levels
286 compared to the results using the vegetation specific thresholds, especially for the 2002 and 2011 wildfires. While the predicted
287 severity using the vegetation specific thresholds could better capture the spatial patterns of fire severity which demonstrate the
288 benefits of applying fixed thresholds to different vegetation in fire severity predictions.

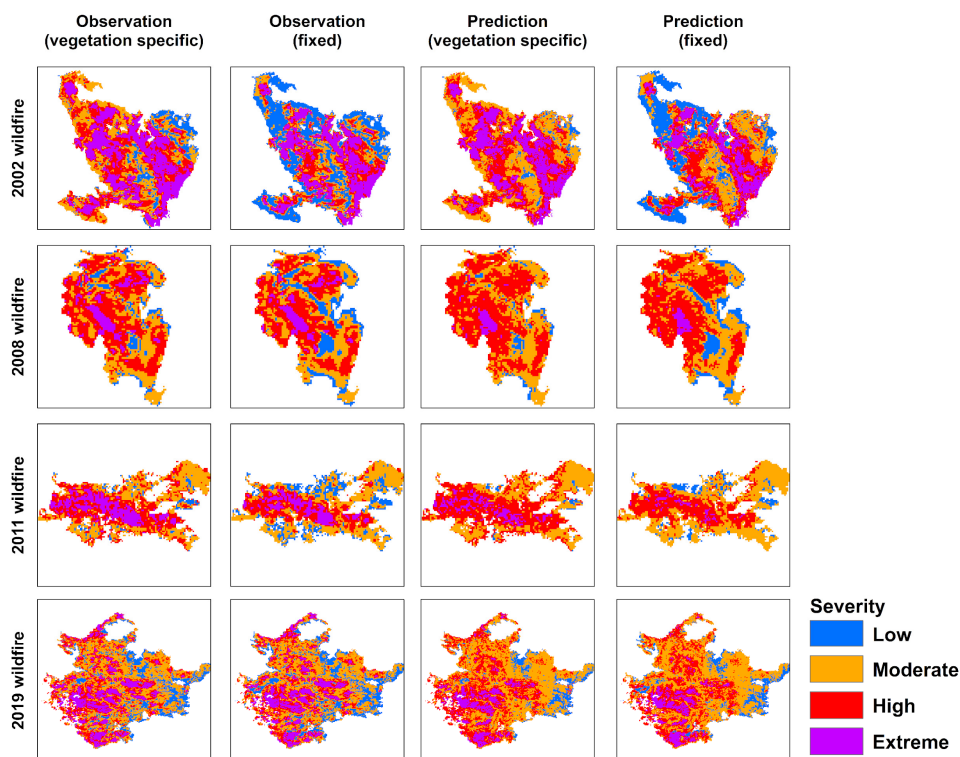


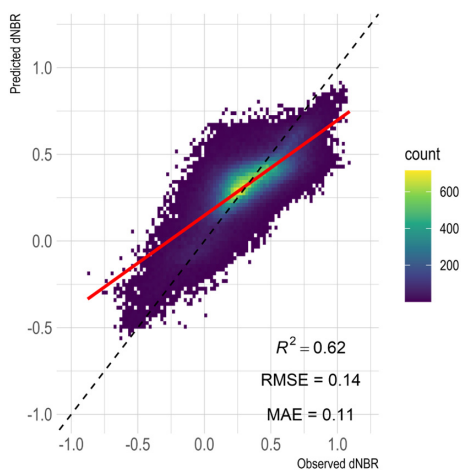
Figure 7. Fire severity classification map based on vegetation specific thresholds and fixed thresholds.

289

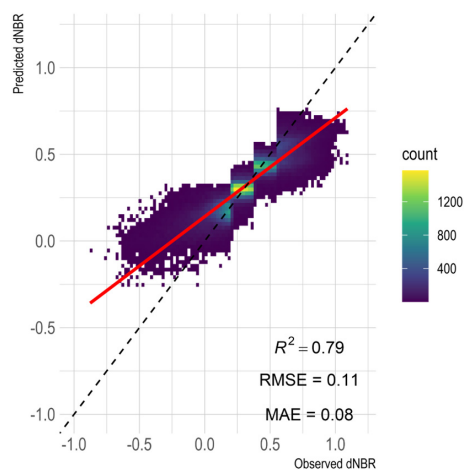
290 To evaluate the model's performance in fire severity prediction, we apply the leave-one-year-out cross-validation method. We
291 validate the fire severity predictions against the observed burn severity derived from Landsat images and compare the
292 predictions based on the RF model with (and without) severity classification method. Figures 8 (a), (b) and (c) display the
293 scatterplots of fire severity prediction against fire severity observations based on RF model without severity classification,
294 with severity classification using the fixed threshold and using the vegetation-specific threshold, respectively. Arguably, the
295 predictions without severity classification show strong underestimation of high fire severity events and overestimation of low
296 burn severity events, with R^2 value of 0.62, RMSE and MAE are 0.14 and 0.11, respectively. The distributions of predictions
297 with severity classification using the fixed threshold do not agree well with observations, though showing higher R^2 (0.79),
298 lower RMSE and MAE values of 0.11 and 0.08, respectively. Predictions with severity classification using the vegetation-



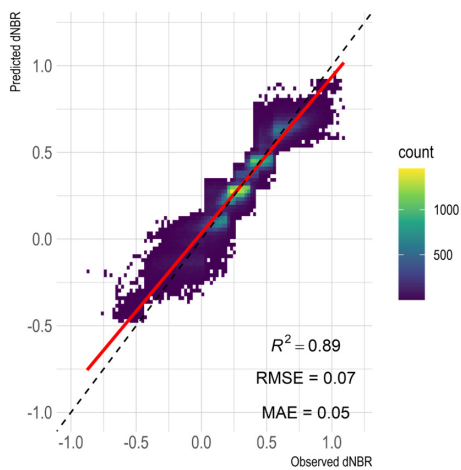
299 specific threshold exhibit better fire severity prediction results for high-, moderate- and low-severity events with improved R^2 ,
300 RMSE and MAE, which are 0.89, 0.07 and 0.05, respectively.



(a)



(b)



(c)



Figure 8. Scatterplots of fire severity prediction against observations based on XGBoost model (a) without severity classification; (b) with severity classification using the fixed threshold; and (c) with severity classification using the vegetation-specific threshold.

301

302 We also evaluate the model's ability of capturing the fire severity dynamics and magnitude in terms of mean fire severity for
303 the selected wildfires. Figure 9 (a) displays the dynamics of predicted fire severity based on RF model with and without severity
304 classification, while Figures 9 (b), (c) and (d) show the dynamics of associated performances of R^2 , RMSE and MAE,
305 respectively. The predictions without severity classification are unable to capture the dynamics of mean fire severity, having
306 the lowest R^2 and highest RMSE and MAE values. While the dynamics of the predicted fire severity with severity classification
307 has better correlation with the observed ones compared to those without severity classification, especially the results with
308 severity classification using the vegetation-specific threshold, which exhibit the best performance of predicting fire severity
309 magnitude with the largest R^2 and lowest RMSE and MAE values. These results indicate that severity classification is an
310 important process to improve the performance of fire severity prediction models.



Figure 9. Time series of (a) mean fire severity, (b) R^2 , (b) RMSE and (c) MAE from 2000 to 2019 based on XGBoost models without severity classification and with severity classification using the fixed and vegetation-specific threshold.

311



312 Figure 10 depicts a summary plot of estimated SHAP values coloured by the feature values, ranked from top to bottom by their
313 importance. It is shown that preNBR is the most important feature in the model, followed by FFDI. The KBDI is also crucial
314 in the model. The topographic factors are also contributing to the model. We can find that having a high preNBR is associated
315 with high and positive values on the model output, indicating the larger preNBR is the prerequisite of more severe wildfire.
316 Similar to the effect of preNBR on the model output, a high FFDI is always associated with high and positive SHAP values,
317 which means the more severe fire weather could lead to more destructive wildfires. Though some high KBDI is found to be
318 associated with negative SHAP values, the KBDI still shows strong positive effect on the model output, reflecting the fact that
319 the dry condition could favour the fire behaviour. Regarding the topography, the large slope and TPI tend to have positive
320 SHAP values, meaning the more severe fire tends to occur in steeper and higher position.
321

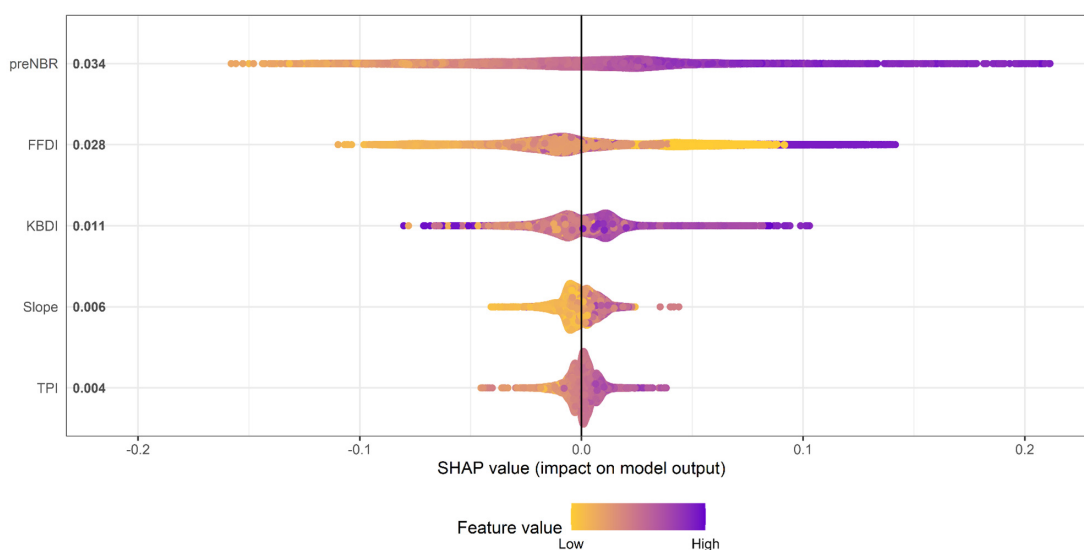


Figure 10. The SHAP values for variables predicting fire severity based on XGBoost model.

322

323 Fig. 11 displays the partial dependence plot (PDP) for each feature in the model. From Figure 11, it can be shown that the
324 preNBR has a strong positive association with the dNBR, implying that dNBR increases with the preNBR rapidly. The FFDI
325 shows a non-monotonic relationship with dNBR, with a decreasing trend observed when it is less than 30, a steady increasing
326 trend between 30 to 65 and significant increasing after it exceeds 65, suggesting that the fire weather dependence is more
327 complex. The weak correlation between KBDI and dNBR, within the range of KBDI lower than 400, indicates that KBDI has
328 nearly no influence when it is below 400. While the positive correlation between KBDI and dNBR, within the range of 400 to
329 600, suggest that the dry condition would intensify the fire severity. However, a declining trend of KBDI is found when it



330 exceeds 600, meaning the impact of KBDI on dNBR becomes weaker. Regarding the slope, a negative association with dNBR
331 is observed when it is below 3, while a positive relationship is found when it exceeds 3. The TPI shows an overall positive
332 association with dNBR. These findings demonstrate that fire severity tends to be higher on steeper slopes and in hilltops.
333

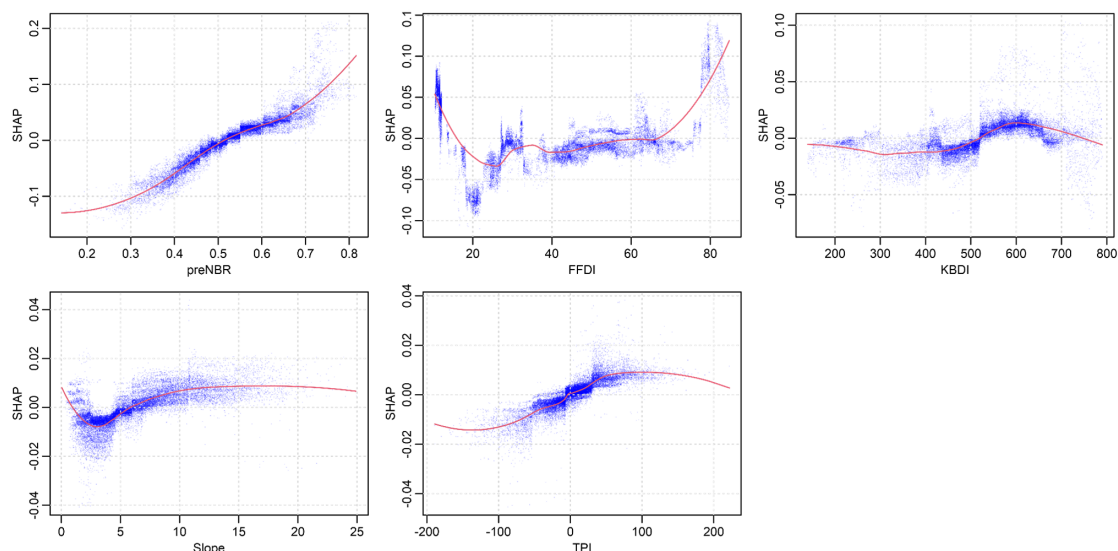


Figure 11. The variation of SHAP values as variables change.

334 5 Discussion

335 This study shows that the proposed predictive technique is capable of providing robust fire severity prediction information,
336 which can be used for forecasting seasonal fire severity and, subsequently, impacts on biodiversity and ecosystems under
337 future projected climate conditions.

338 We find that the RF method is effective in classifying fire events into different levels of fire severity and XGBoost method is
339 a useful method to characterise the relationships between fire severity and explanatory variables (e.g., preNBR, FFDI, KBDI,
340 slope and TPI). Fire severity is a complex function of explanatory variables gradients and these relationships may vary in
341 different vegetation type and severity levels. The preNBR, an approximation of the pre-fire vegetation condition, plays an
342 important role in classification and prediction, as the change in NBR pre- and post-fire, i.e. dNBR, will be dependent on both
343 the condition of the vegetation before the fire and the degree of change to vegetation after the fire. The preNBR, indicating the
344 pre-fire vegetation condition, might be related to the pre-fire drought. For example, drought reduces the water content of
345 foliage (Choat et al. 2018), thus reducing preNBR, so the maximum absolute change in NBR (dNBR) possible might be smaller



346 during a drought year than a non-drought year. The FFDI is found to be important in fire severity classification and prediction.
347 The meteorological conditions are proven to be the most influential predictors in determining the magnitude of fire severity
348 (Clarke et al., 2014; Bowman et al., 2021). The FFDI is the index of fire weather severity during the fire season thus is workable
349 in determining the potential burn severity level. KBDI is another important variable in fire severity classification. It is known
350 that drought can create conditions that favour severe fires (Abram et al. 2021) and that the combined effects of fire and drought
351 can contribute to plant population declines (Gallagher et al. 2022; Nolan et al. 2021) and ecosystem transformation (Keith et al.
352 al. 2022). Severe drought conditions also directly contribute to forest flammability (Nolan et al. 2020). More importantly, the
353 frequency, intensity and duration of drought conditions are projected to shift under future climates (Ukkola et al. 2020). These
354 changes in drought regimes will likely be associated with increases in the size, frequency and severity of fires (Abram et al.
355 2021). TPI and slope, as important topographic factors, also have considerable influence on low fire severity. For example,
356 Bradstock et al. (2010) found burn severity is lower in valleys, probably due to effects of wind protection and higher fuel
357 moisture in moderating fire behaviour. Barker et al. (2018) found that the probability of low severity increased with slope. In
358 this study, we find that fire severity tends to be higher on steeper slopes and higher position, this might be that steep slopes
359 can intensify fire behaviour by creating a chimney effect that draws in air and accelerates the fire (Andrews and Bradshaw,
360 2012; Jolly et al., 2015; Seginer and Brandl, 2007.). Besides, higher elevations generally have lower air pressure and reduced
361 humidity, which helps fire burn more intensely (Abatzoglou and Kolden, 2011; Holden et al., 2018). Additionally, vegetation
362 on steep slopes can be thicker and more continuous, providing more fuel for the fire (Collins et al., 2009; Pausas and Fernández-
363 Muñoz, 2012).

364 The introduction of vegetation specific thresholds is proven to be beneficial for fire severity classification. The range of dNBR
365 varies significantly with vegetation types, and thus applying a fixed threshold in dNBR would lead to a large amount of
366 misclassification in fire severity levels. This kind of mis-classification error is mitigated by using vegetation specific thresholds
367 in dNBR. The vegetation type also plays an important role in the RF model. The relative influence of vegetation type is larger
368 than the topographic factors while the deviation of vegetation type is the largest in the meantime. The relative influence of
369 vegetation type and the deviation changes with the number of vegetation types and its fractions in the fire event. For example,
370 five vegetation types were affected in the 2002 wildfire, and the fractions of vegetation types are: dry sclerophyll forests
371 (shrubby subformation) (30%), grassy woodlands (31 %), wet sclerophyll forests (grassy subformation) (23%), dry sclerophyll
372 forests (Shrub/grass subformation) (14%) and grasslands (2%). While in the 2019 wildfire, seven vegetation types were
373 affected, dry sclerophyll forests (shrubby subformation) accounts for 92% of the burn area. The relative influence of vegetation
374 type in the 2002 wildfire is around 10% while only 5% in the 2019 wildfire. This could also explain why no significant
375 differences are found between fire severity maps using vegetation specific thresholds and fixed thresholds in the 2019 wildfire.
376 Since more than 90% of the burn area in the 2019 wildfire is covered by dry sclerophyll forests (shrubby subformation) and
377 the fixed thresholds are adopted from the thresholds of dry sclerophyll forests (shrubby subformation), the fire severity
378 classification for 2019 wildfire is almost equal to the fire severity classification for dry sclerophyll forests (shrubby
379 subformation).



380 This study develops a predictive technique which is capable of providing robust fire severity classification and prediction
381 information for historical events, which also has the potential to forecast the seasonal fire severity. The input variables to the
382 model could be obtained from other forecast models: fire weather related variables can be extracted from the Weather Research
383 and Forecasting (WRF) model. The preNBR has the seasonality characteristics, which can be predicted based on the historical
384 preNBR time series. The vegetation type and topographic factors are static variables, while the variables for calculating FFDI
385 and KBDI, e.g., wind speed, relative humidity, precipitation, air temperature, are available from WRF outputs. Quick
386 assessment of fire severity for wildfires are accessible based on the proposed predictive technique, once the burn area are
387 derived from the burn area prediction models (Alkhatib, 2014; Castelli et al., 2015) or monitoring products (e.g., MODIS
388 Burned Area Product, MCD64A1)

389 6 Conclusions

390 This study introduces the vegetation specific thresholds in fire severity classification for wildfires over NSW, Australia. We
391 use the pre-fire season drought conditions, topography, and the fire season meteorological conditions as input to build the
392 predictive model and the performances are validated by EXtreme Gradient Boosting (XGBoost) to predict the fire severity,
393 proxied by dNBR.

394 Using the vegetation specific thresholds we could improve the classification accuracy in fire severity levels. Specifically, using
395 a leave-one-out cross-validation, the severity classification results showed an improved classification accuracy of 0.75 based
396 on the proposed vegetation specific thresholds, compared to those based on fixed thresholds (0.69). The predictive performance
397 of XGBoost model is improved as well based on the classification results, with determination coefficient (R^2), mean absolute
398 error (MPE) and root mean square error (RMSE) values of 0.89, 0.05, and 0.07, respectively. We show that the preNBR is the
399 most important variable in fire severity classification and prediction, followed by FFDI and KBDI. The PDP of FFDI and
400 KBDI indicate that the likelihood of high severity increases when weather and drought conditions become more severe. From
401 the responses of dNBR to topographic factors, the probability of high severity increases with slope and elevation. The role of
402 vegetation type in fire severity prediction becomes more important for large fires where more diverse vegetation is affected.

403 The results demonstrate that the prediction technique performs well predicting fire severity of historic fires (2000-2019) in the
404 Australian state of NSW, while it also shows the potential to be applicable for seasonal fire severity forecasts, owing to the
405 availability of the predictor variables in seasonal forecasting outputs. With the expected increase in wind speed, temperature
406 and drought conditions exhibited in future climate projections, this prediction technique can also be used to evaluate the
407 variation of fire severity under climate change.

408

409 **Author contributions:** Kang He: Data curation, Visualization, Writing-Original draft preparation. Xinyi Shen: Supervision,
410 Methodology, Writing- Reviewing and Editing. Emmanouil N. Anagnostou: Supervision, Methodology, Writing-Reviewing
411 and Editing Cory Merow: Methodology, Writing-Reviewing and Editing. Efthymios Nikolopoulos: Data curation, Writing-



412 Reviewing and Editing. Rachael Gallagher: Data curation, Writing-Reviewing and Editing Feifei Yang: Methodology,
413 Writing- Reviewing and Editing.

414

415 **Competing interests:** The contact author has declared that none of the authors has any competing interests.

416

417 **Acknowledgements:** This research was supported by National Science Foundation HDR award entitled “Collaborative
418 Research: Near term forecast of Global Plant Distribution Community Structure, and Ecosystem Function”. Kang He received
419 the support of China Scholarship Council for four years' Ph.D. study in University of Connecticut (under grant agreement no.
420 201906320068).

421

422 **References**

423 Abatzoglou, J. T., Williams, A. P., & Barbero, R. (2019). Global emergence of anthropogenic climate change in fire weather
424 indices. *Geophysical Research Letters*, 46(1), 326-336.

425 Abatzoglou, J.T. and Kolden, C.A., 2011. Climate change in western US deserts: potential for increased wildfire and invasive
426 annual grasses. *Rangeland Ecology & Management*, 64(5), pp.471-478.

427 Abram, N. J., Henley, B. J., Sen Gupta, A., Lippmann, T. J., Clarke, H., Dowdy, A. J., ... & Boer, M. M. (2021). Connections
428 of climate change and variability to large and extreme forest fires in southeast Australia. *Communications Earth &
429 Environment*, 2(1), 1-17.

430 Alkhatib, A.A., 2014. A review on forest fire detection techniques. *International Journal of Distributed Sensor Networks*,
431 10(3), p.597368.

432 Andrews, P. L., & Bradshaw, L. S. (2012). The effects of slope and aspect on fire behavior. In *Fire in California's ecosystems*
433 (pp. 153-171). University of California Press. <https://doi.org/10.1525/california/9780520278806.003.0011>

434 Archibald, S., Lehmann, C. E., Gómez-Dans, J. L., & Bradstock, R. A. (2013). Defining pyromes and global syndromes of
435 fire regimes. *Proceedings of the National Academy of Sciences*, 110(16), 6442-6447.

436 Barker, J. W., & Price, O. F. (2018). Positive severity feedback between consecutive fires in dry eucalypt forests of southern
437 Australia. *Ecosphere*, 9(3), e02110.

438 Boby, L. A., Schuur, E. A., Mack, M. C., Verbyla, D., & Johnstone, J. F. (2010). Quantifying fire severity, carbon, and nitrogen
439 emissions in Alaska's boreal forest. *Ecological Applications*, 20(6), 1633-1647.

440 Bowman, D. M., Williamson, G. J., Gibson, R. K., Bradstock, R. A., & Keenan, R. J. (2021). The severity and extent of the
441 Australia 2019–20 Eucalyptus forest fires are not the legacy of forest management. *Nature Ecology & Evolution*, 5(7), 1003-

442 1010.



- 443 Bradstock, R. A., Hammill, K. A., Collins, L., & Price, O. (2010). Effects of weather, fuel and terrain on fire severity in
444 topographically diverse landscapes of south-eastern Australia. *Landscape Ecology*, 25(4), 607-619.
- 445 Breiman, L. (2001). Random forests. *Machine learning*, 45(1), 5-32.
- 446 Castelli, M., Vanneschi, L. and Popovič, A., 2015. Predicting burned areas of forest fires: an artificial intelligence approach.
447 *Fire ecology*, 11(1), pp.106-118.
- 448 Chen, T. and Guestrin, C., 2016, August. Xgboost: A scalable tree boosting system. In *Proceedings of the 22nd acm sigkdd
449 international conference on knowledge discovery and data mining* (pp. 785-794).
- 450 Chen, T., He, T., Benesty, M., Khotilovich, V., Tang, Y., Cho, H., Chen, K., Mitchell, R., Cano, I. and Zhou, T., 2015. Xgboost:
451 extreme gradient boosting. *R package version 0.4-2*, 1(4), pp.1-4.
- 452 Clarke, H., Tran, B., Boer, M. M., Price, O., Kenny, B., & Bradstock, R. (2019). Climate change effects on the frequency,
453 seasonality and interannual variability of suitable prescribed burning weather conditions in south-eastern Australia.
454 *Agricultural and Forest Meteorology*, 271, 148-157.
- 455 Clarke, P. J., Knox, K. J., Bradstock, R. A., Munoz-Robles, C., & Kumar, L. (2014). Vegetation, terrain and fire history shape
456 the impact of extreme weather on fire severity and ecosystem response. *Journal of Vegetation Science*, 25(4), 1033-1044.
- 457 Collins, B. M., Kelly, M., Van Wagtenonk, J. W., & Stephens, S. L. (2007). Spatial patterns of large natural fires in Sierra
458 Nevada wilderness areas. *Landscape Ecology*, 22(4), 545-557.
- 459 Collins, B. M., Miller, J. D., Thode, A. E., Kelly, M., & van Wagtenonk, J. W. (2009). Interactions among wildland fires in
460 a long-established Sierra Nevada natural fire area. *Ecosystems*, 12(1), 114-128. <https://doi.org/10.1007/s10021-008-9211-1>
- 461 Collins, L., Bennett, A. F., Leonard, S. W., & Penman, T. D. (2019). Wildfire refugia in forests: Severe fire weather and
462 drought mute the influence of topography and fuel age. *Global Change Biology*, 25(11), 3829-3843.
- 463 Collins, L., Bradstock, R. A., & Penman, T. D. (2013). Can precipitation influence landscape controls on wildfire severity? A
464 case study within temperate eucalypt forests of south-eastern Australia. *International Journal of Wildland Fire*, 23(1), 9-20.
- 465 Dillon, G. K., Holden, Z. A., Morgan, P., Crimmins, M. A., Heyerdahl, E. K., & Luce, C. H. (2011). Both topography and
466 climate affected forest and woodland burn severity in two regions of the western US, 1984 to 2006. *Ecosphere*, 2(12), 1-33.
- 467 Dowdy, A. J., Mills, G. A., Finkele, K., & De Groot, W. (2009). Australian fire weather as represented by the McArthur forest
468 fire danger index and the Canadian forest fire weather index (p. 91). Melbourne: Centre for Australian Weather and Climate
469 Research.
- 470 Eidenshink, J., Schwind, B., Brewer, K., Zhu, Z.L., Quayle, B. and Howard, S., 2007. A project for monitoring trends in burn
471 severity. *Fire ecology*, 3(1), pp.3-21.
- 472 Fang, L., Yang, J., White, M., & Liu, Z. (2018). Predicting potential fire severity using vegetation, topography and surface
473 moisture availability in a Eurasian boreal forest landscape. *Forests*, 9(3), 130.
- 474 Gallagher, R. V., Allen, S. P., Mackenzie, B. D., Keith, D. A., Nolan, R. H., Rumpff, L., ... & Auld, T. D. (2022). An integrated
475 approach to assessing abiotic and biotic threats to post-fire plant species recovery: Lessons from the 2019–2020 Australian
476 fire season. *Global Ecology and Biogeography*.



- 477 Gallagher, R. V., Allen, S., Mackenzie, B. D., Yates, C. J., Gosper, C. R., Keith, D. A., ... & Auld, T. D. (2021). High fire
478 frequency and the impact of the 2019–2020 megafires on Australian plant diversity. *Diversity and Distributions*, 27(7), 1166-
479 1179.
- 480 García, M. L., & Caselles, V. (1991). Mapping burns and natural reforestation using Thematic Mapper data. *Geocarto*
481 *International*, 6(1), 31-37.
- 482 Hammill, K. A., & Bradstock, R. A. (2006). Remote sensing of fire severity in the Blue Mountains: influence of vegetation
483 type and inferring fire intensity. *International Journal of Wildland Fire*, 15(2), 213-226.
- 484 Harris, L., & Taylor, A. H. (2015). Topography, fuels, and fire exclusion drive fire severity of the Rim Fire in an old-growth
485 mixed-conifer forest, Yosemite National Park, USA. *Ecosystems*, 18(7), 1192-1208.
- 486 Harris, L., & Taylor, A. H. (2017). Previous burns and topography limit and reinforce fire severity in a large wildfire.
487 *Ecosphere*, 8(11), e02019.
- 488 Hennessy, K., Lucas, C., Nicholls, N., Bathols, J., Suppiah, R., & Ricketts, J. (2005). Climate change impacts on fire-weather
489 in south-east Australia. Climate Impacts Group, CSIRO Atmospheric Research and the Australian Government Bureau of
490 Meteorology, Aspendale.
- 491 Holden, Z. A., Morgan, P., & Evans, J. S. (2009). A predictive model of burn severity based on 20-year satellite-inferred burn
492 severity data in a large southwestern US wilderness area. *Forest Ecology and Management*, 258(11), 2399-2406.
- 493 Holden, Z.A., Swanson, A., Luce, C.H., Jolly, W.M., Maneta, M., Oyler, J.W., Warren, D.A., Parsons, R. and Affleck, D.,
494 2018. Decreasing fire season precipitation increased recent western US forest wildfire activity. *Proceedings of the National*
495 *Academy of Sciences*, 115(36), pp.E8349-E8357.
- 496 Hudak, A. T., Ottmar, R. D., Vihnanek, R. E., Brewer, N. W., Smith, A. M., & Morgan, P. (2013). The relationship of post-
497 fire white ash cover to surface fuel consumption. *International Journal of Wildland Fire*, 22(6), 780-785.
- 498 Jolly, W. M., Cochrane, M. A., Freeborn, P. H., Holden, Z. A., Brown, T. J., Williamson, G. J., & Bowman, D. M. J. S. (2015).
499 Climate-induced variations in global wildfire danger from 1979 to 2013. *Nature Communications*, 6, 7537.
500 <https://doi.org/10.1038/ncomms8537>
- 501 Keeley, J. E. (2009). Fire intensity, fire severity and burn severity: a brief review and suggested usage. *International journal*
502 *of wildland fire*, 18(1), 116-126.
- 503 Keetch, J. J., & Byram, G. M. (1968). A drought index for forest fire control. USDA Forest Service Research Paper SE-38.
504 Asheville, NC.
- 505 Keith, D. A. (2004). Ocean shores to desert dunes: the native vegetation of New South Wales and the ACT. Department of
506 Environment and Conservation (NSW).
- 507 Keith, D. A., Allen, S. P., Gallagher, R. V., Mackenzie, B. D., Auld, T. D., Barrett, S., ... & Tozer, M. G. (2022). Fire-related
508 threats and transformational change in Australian ecosystems. *Global Ecology and Biogeography*.
- 509 Key, C.H. and Benson, N.C., 2006. Landscape assessment (LA). FIREMON: Fire effects monitoring and inventory system,
510 164, pp.LA-1.



- 511 Lentile, L. B., Holden, Z. A., Smith, A. M., Falkowski, M. J., Hudak, A. T., Morgan, P., ... & Benson, N. C. (2006). Remote
512 sensing techniques to assess active fire characteristics and post-fire effects. *International Journal of Wildland Fire*, 15(3), 319-
513 345.
- 514 Lutes, D.C., Keane, R.E., Caratti, J.F., Key, C.H., Benson, N.C., Sutherland, S. and Gangi, L.J., 2006. FIREMON: Fire effects
515 monitoring and inventory system. Gen. Tech. Rep. RMRS-GTR-164. Fort Collins, CO: US Department of Agriculture, Forest
516 Service, Rocky Mountain Research Station. 1 CD., 164.
- 517 McArthur AG (1967). Fire behaviour in eucalypt forests. Commonwealth of Australia, Forest and Timber Bureau Leaflet 107.
518 (Canberra, ACT, Australia)
- 519 Miller, J. D., Knapp, E. E., Key, C. H., Skinner, C. N., Isbell, C. J., Creasy, R. M., & Sherlock, J. W. (2009). Calibration and
520 validation of the relative differenced Normalized Burn Ratio (RdNBR) to three measures of fire severity in the Sierra Nevada
521 and Klamath Mountains, California, USA. *Remote Sensing of Environment*, 113(3), 645-656.
- 522 Morgan, P., Keane, R. E., Dillon, G. K., Jain, T. B., Hudak, A. T., Karau, E. C., ... & Strand, E. K. (2014). Challenges of
523 assessing fire and burn severity using field measures, remote sensing and modelling. *International Journal of Wildland Fire*,
524 23(8), 1045-1060.
- 525 Nolan, R. H., Boer, M. M., Collins, L., Resco de Dios, V., Clarke, H. G., Jenkins, M., ... & Bradstock, R. A. (2020). Causes
526 and consequences of eastern Australia's 2019-20 season of mega-fires. *Global change biology*.
- 527 Nolan, R. H., Collins, L., Leigh, A., Ooi, M. K., Curran, T. J., Fairman, T. A., ... & Bradstock, R. (2021). Limits to post-fire
528 vegetation recovery under climate change. *Plant, cell & environment*, 44(11), 3471-3489.
- 529 Pausas, J. G., & Fernández-Muñoz, S. (2012). Fire regime changes in the Western Mediterranean Basin: from fuel-limited to
530 drought-driven fire regime. *Climatic Change*, 110(1-2), 215-226. <https://doi.org/10.1007/s10584-011-0060-6>
- 531 Seginer, I., Körner, C., & Brandl, H. (2007). Topography and microclimate of exposed sites in a dry alpine valley. *Arctic,*
532 *Antarctic, and Alpine Research*, 39(3), 463-469. [https://doi.org/10.1657/1523-0430\(2007\)39\[463:TAMOES\]2.0.CO;2](https://doi.org/10.1657/1523-0430(2007)39[463:TAMOES]2.0.CO;2)
- 533 Shine, J. (2020). Statement regarding Australian bushfires. [https://www.science.org.au/news-and-events/news-and-media-](https://www.science.org.au/news-and-events/news-and-media-releases/australian-bushfires-why-they-are-unprecedented)
534 [releases/australian-bushfires-why-they-are-unprecedented](https://www.science.org.au/news-and-events/news-and-media-releases/australian-bushfires-why-they-are-unprecedented). Accessed 4 February 2020.
- 535 Soverel, N. O., Perrakis, D. D., & Coops, N. C. (2010). Estimating burn severity from Landsat dNBR and RdNBR indices
536 across western Canada. *Remote Sensing of Environment*, 114(9), 1896-1909.
- 537 Speer, M. S., Wiles, P., & Pepler, A. (2009). Low pressure systems off the New South Wales coast and associated hazardous
538 weather: establishment of a database. *Australian Meteorological and Oceanographic Journal*, 58(1), 29.
- 539 Takeuchi, W., Darmawan, S., Shofiyati, R., Khiem, M. V., Oo, K. S., Pimple, U., & Heng, S. (2015, October). Near-real time
540 meteorological drought monitoring and early warning system for croplands in asia. In *Asian Conference on Remote Sensing*
541 *2015: Fostering Resilient Growth in Asia (Vol. 1, pp. 171-178)*.
- 542 Tran, B.N., Tanase, M.A., Bennett, L.T. and Aponte, C., 2018. Evaluation of spectral indices for assessing fire severity in
543 Australian temperate forests. *Remote sensing*, 10(11), p.1680.



544 Ukkola, A. M., De Kauwe, M. G., Roderick, M. L., Abramowitz, G., & Pitman, A. J. (2020). Robust future changes in
545 meteorological drought in CMIP6 projections despite uncertainty in precipitation. *Geophysical Research Letters*, 47(11),
546 e2020GL087820.

547 Wang, C., & Glenn, N. F. (2009). Estimation of fire severity using pre-and post-fire LiDAR data in sagebrush steppe
548 rangelands. *International Journal of Wildland Fire*, 18(7), 848-856.

549

550

551

552

553